IJISET - International Journal of Innovative Science, Engineering & Technology, Vol. 09 Issue 10, October 2022
ISSN (Online) 2348 – 7968 | Impact Factor – 6.72
www.ijiset.com

Land Use Change Modeling Using Gis and Ca-Markov Model, Case Study Of Djibi Basin (Abidjan- Côte D'ivoire)

Anzoumanan Kamagaté [1], Blaise Koffi Yao[2], Kouakou Koffi Aboudellaziz [3], Djakaridja Ouafoundanhan Coulibaly [4]

[1]Training and Research Unit for Marine Sciences, University of San-Pedro, City: San Pedro, Ivory Coast, email: anzokam@gmail.com; anzoumanan.kamagate@usp.edu.ci, Tel: (+225) 07 07 73 35 83

[2]Training and Research Unit for Earth Sciences and Mining Resources, Soil, Water and Geomaterials Laboratory, University of Félix Houphouët-Boigny, Abidjan, Ivory Coast

[3] Department of Geosciences, University of Peleforo Gon Coulibaly, Korhogo, Ivory Coast

[4]Training and Research Unit for Earth Sciences and Mining Resources, Soil, Water and Geomaterials Laboratory, University of Félix Houphouët-Boigny, Abidjan, Ivory Coast

Abstract

Changes in land use land cover relevant to anthropogenic activities have significantly impact the ecosystem. The aims of this study is to simulate land use change in Djibi watershed (Abidjan-Côte d'Ivoire) by 2050 using the CA_Markov model.

In Idrisi TerrSet software, modules like CA-MARKOV, and GIS were used for modeling and land-use change projecting, a recent and innovative approach well known in scientific community, which indicates our interest of this tool for the purpose of our work.

The predicting result indicates that from 1987 to 2019, the croplands would decrease and have given way to the urban areas. Land use change scenario made from 2019-2050 was simulated with Kappa statistics (K=0.87).

Furthermore, the study reveals that biophysical and socio-economic factors (population density) are the main causes of the regression of the natural landscape. This regression of natural resources seems to continue in the future with current land practices.

Keywords: GIS, CA-Markov model, land-use change, Idrisi, Djibi watershed

1. Introduction

Agricultural areas and settlements is increasing, that result to woodland reduction [13] and destabilization of soil structure [2]. The outskirts of big cities are increasingly urbanized, and that resulted to a significant of natural environments which has a strong impact on watercourses regime in peri-urban catchment areas [8].

For all these reasons, land-use change is increasingly attracted huge attention of researchers and is currently being taken into account by the research conducted on "Global change" [3]. Like developing countries, Côte d'Ivoire's economy is heavily dependent on the agricultural and forestry sector, leading to rapid decrease in forest area [26] and land degradation. In fact, the forest area has decreased from about 14 million hectares in 1912 to almost 2 million hectares in 2000 [20] and [12]. Abidjan's land cover in general and the Djibi watershed in particular has not escaped this deforestation because of anthropic pressures due to its urbanization. Several methods have been applied for land cover study with varying levels of effectiveness ([23] and [22]. We can mention, diachronic and multi-date analysis of land use is one of the most used, because it takes into account the spatial distribution of changes [16].

Remote sensing (RS) and geographic information systems (GIS) have been popularly adopted as essential and useful tools in obtaining accurate spatial data of LULC and quantifying the alternations of spatial data. The application of the CA-Markov model in predicting LULC changes has conveniences due to its powerful replication, and it is used for mapping LULC changes providing good performance regardless of dynamic modeling efficiently; high productivity with data, simple analysis; and capacity to detect transitions between land use classes [31].

In Idrisi TerrSet software, modules like CA-MARKOV, and GIS were used for modeling and land-use change projecting, a recent and innovative approach well known in scientific community, which indicates our interest of this tool for the purpose of our study.

Thus, the present study aims to simulate dynamic of land use change in the Djibi watershed (Abidjan-Côte d'Ivoire) by 2050 using the CA-Markovian model.

2. Study area

Djibi watershed is located in the Northeast part of Abidjan between Latitudes of 5°23 and 5°29 North and Longitudes of 3°55 and 4°03 West in geographic coordinate system (WGS 84, zone 30 N) (Fig. 1). It is limited in the north part by Anyama in the south by Bingerville [19].

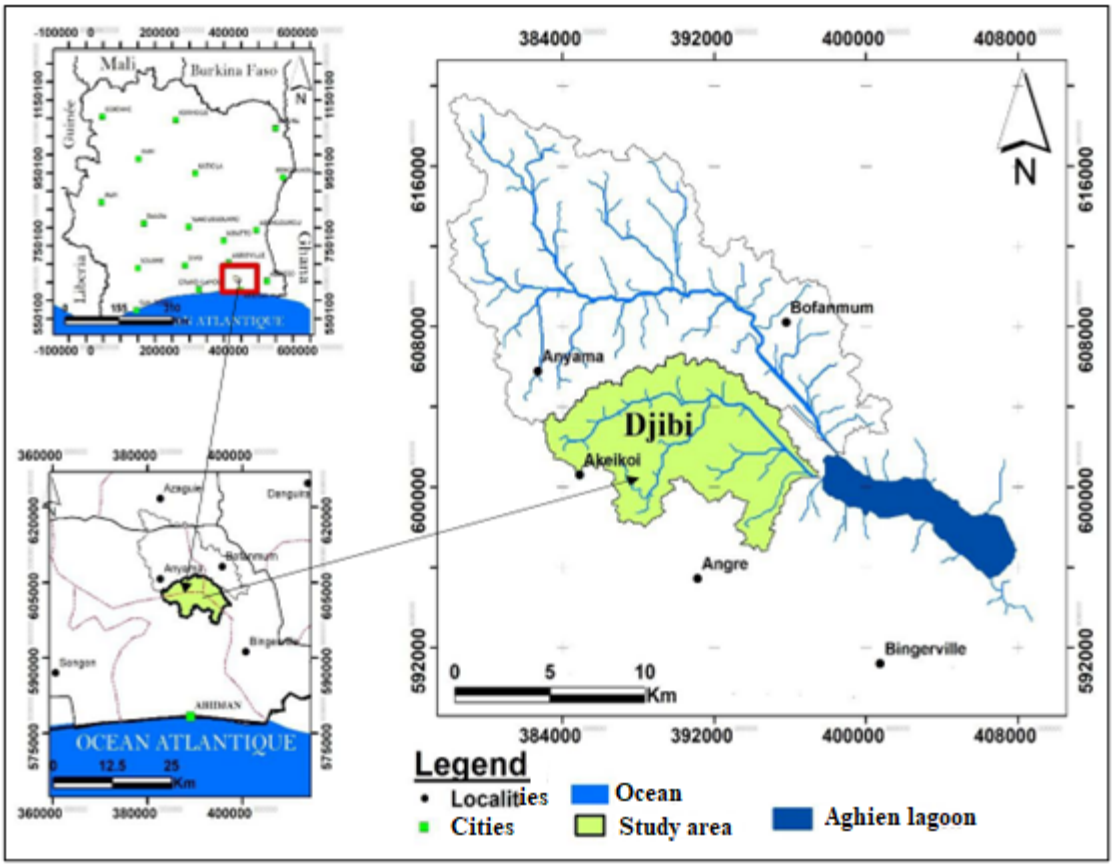

Fig. 1 : Location of the study area

The study area has an equatorial transition climate (Attieen Climat) or sub-equatorial climate divided into two (2) rainy seasons (long rainy season from May to july and short rainy season from October to November) and two (2) dry season (long dry season from December to April and short dry season from august to september.

Annual rainfall varies from 1202.8 mm to 1413 mm. Agriculture is the main economic activity in the catchment. Export crops such as oil palm and rubber are grown.

3. Materials and Methods

3.1. Data Acquisition

The research used USGS satellite images from Landsat TM (Thematic Mapper), ETM+ (Enhancement Thematic Mapper plus) and OLI-TIRS sensors. These satellite images were captured on 12 January 1987 for the TM sensor, on 24 January 2002 for the ETM+ sensor and on 20 January for the OLI-TIRS sensor. These months correspond to the dry season when cloud cover and cloudiness are reduced. These 30m resolution images are provided free of charge on the USGS website

(http: //earthexplorer.gov). The study area is located on scene (Path/Row) 196 /056. The Landsat images were supplemented by GPS ground surveys. Sample points were used to classify the images. Various software packages were used for processing the satellite images. ENVI 5.1 for digital image processing; IDRISI TerrSet, for change detection and implementation of predictive land use modelling. QGIS 3.16 software was used for the elaboration of the maps and Google Earth Pro was used to visualise the landscape of the catchment area in order to be able to identify the types of land use.

3.2. Methods

3.2.1. Landsat images pre-processing

Landsat TM, ETM+ and OLI images used in this study are geometrically corrected, georeferenced and projected in the UTM system, WGS84, zone 30 N. Only radiometric corrections have been process on this images. This correction consists of converting the pixel values of the digital count into reflectance values. The "Radiometric Calibration" tool in ENVI 5.1 was used to make this correction. In addition, to correct for any atmospheric bias, the Dark Object Substaction tool was used to make this correction.

3.2.2. Landsat images Digital processing

3.2.2.1. Spectral Enhancement:

Color Enhancement combining 3/4/7 bands from Landsat TM (1986), 5/4/2 bands from Landsat ETM+ (2000) and 2/5/6 band for OLI-TIRS (2019) [15] and [28] were produced. The aims is to summarize information for good discrimination of land use units. In addition, the visual interpretation of the images, which establish relationship between the field and the image allowed us to identify details such as: water, bare soil, rubber plantations, palm trees and degraded forests, habitats, and food crops and fallow land on the different images.

3.2.2.2. Classification and validation

In a broad sense, image classification is defined as the process of categorizing all pixels in an image or raw remotely sensed satellite data to obtain a given set of labels or land cover themes. In some instances, the classification itself may be the object of the analysis. For example, classification of land use from remotely sensed data produces a map like image as the final product of the analysis. Hence the image classification forms an important tool for examination of the digital images. This step is called training. Once trained, the classifier is then used to attach labels to all the image pixels according to the trained parameters. The quality of a supervised classification depends on the quality of the training sites, the most commonly used supervised classification is maximum likelihood classification.

Supervised classification was apply in case of this study. It is essential tool form ENVI 5.1 software used for extracting quantitative information from remotely sensed image data. Using this method, the analyst has available sufficient known pixels to generate representative parameters for each class of interest in the images and by properly considering the spatial context information. Experimental results confirmed the effectiveness of the proposed system.

The training plot samples selection; the description and information of the different classes. The Maximum Likelihood algorithm based on Bayes' rule was chosen for images classification. It is a method that calculates the probability of a pixel belonging to a given class rather than another [21]. The pixels will be assigned to the class for which the probability is highest. However, if this probability does not reach the expected threshold, the pixel is classified as "unknown". The quality of the classification obtained was evaluated using the parameters calculated by the confusion matrix, i.e. the overall accuracy and the Kappa coefficient [6], [15] and [4]. The last stage of image processing resulted in the design of land use maps and, above all, the development of statistics. It includes operations such as vectorisation, integration of the results in GIS and production of the maps. Vectorisation consisted of the conversion of classified images from raster mode to vector mode (polygons) in order to facilitate their management in the GIS analysis software.

3.2.2.3. Land use change Analysis in Djibi watershed

Changes analysis from 1987 to 2019 was done by a post-classification comparison. It produces a change detection matrix resulting from the comparison between the pixels of two classifications between two dates [15]. From this situation, the overall rate of change (Tg) and the average annual rate of spatial expansion (Tc) were calculated. The calculation of the annual rate of change (Tc) and the overall rate of change (Tg), commonly used in land use change studies, is based on the following formula [11] and [17]:

$Tc = [(S2 / S1)1/t - 1] \times 100$ (Eq.1)

$Tg = ((S2 - S1) / S1) \times 100$ (Eq.2)

Où : Tc = Annual change's rate (%) ; Tg = global change's rate

S1 = class area on the date t1; S2 = class area on the date t2 (t2 > t1)

t = years number between the two dates.

Change rate Analysis values shows that positive values indicate "progression" and negative values indicate "regression". Values close to zero indicate that the class is relatively "stable".

3.2.3. Land use change simulation in Djibi catchment area by 2050 using the Markov chain model

3.2.3.1. Model choice

Several models for land cover simulation were used and the most commonly used are CA_Markov, LCM, Dinamica EGO and CLUE-S. From a wide range of land cover simulation model approaches, CA_Markov model has been chose [9] for its performance, efficiency, multi-scale potential and spatially explicit procedure based on raster data.

CA-Markov is a combination of Cellular Automata (CA) and the Markov module for land use prediction. CA-Markov model integrated with GIS is considered to be an appropriate approach to model temporal and spatial evolution of land use change [25]. Markov transition chains can be described as follows [18]:

Π(t+1) = P^n.Π(t) (Eq.3)

with **Π(t),** Actual system step at **t**; **Π (t+1)** is the system step in time **t+1** and $\mathbf{P^n}$, the possible steps to occur, which described the probability transition matrix.

This matrix shows the possibility to determine a stable or step i changing to step j during the passage t à t+1.

3.2.3.2. Model calibration and validation

In order to simulate the dynamics of land use at a later (2050), the model must first be calibrated on known data. As the 2019 image is the most recent, it was the subject of a first test simulation, calibrated by two earlier dates (1987 and 2002). The 1987 and 2002 images are used as a basis for extrapolating future land use quantities. This is a linear extrapolation, as the simulation is based on two points in time to calibrate the model. According to [30], calibration is the estimation and adjustment of model parameters and constraints to improve the fit between model outputs and a data set. This step is fundamental, as the quality of the results obtained will depend on the correct parameterization of the model.

For the validation, the result of the land use simulation of 2019 is compared to the land use map of 2019 resulting from the classification. [30] show the interest of such a comparison between these maps as it would avoid the subjectivity and lack of precision of a purely visual comparative approach between a reference map and the simulation. This simulation time was defined to escape the limitations of the model, as it is a spatially unexplicit approach and therefore very little used even in empirical studies of urban sprawl simulation [24]. After a visual comparison, a further analysis is made by calculating Kappa indices assessing the quality of the prediction in terms of location. This evaluation produces Kappa agreement indices: (i) Kappa for location of grid-cell level location (Klocation) and (ii) Kstandard to determine an overall success rate [29] and [5]. Methodology of land use mapping is presented in Figure 2.

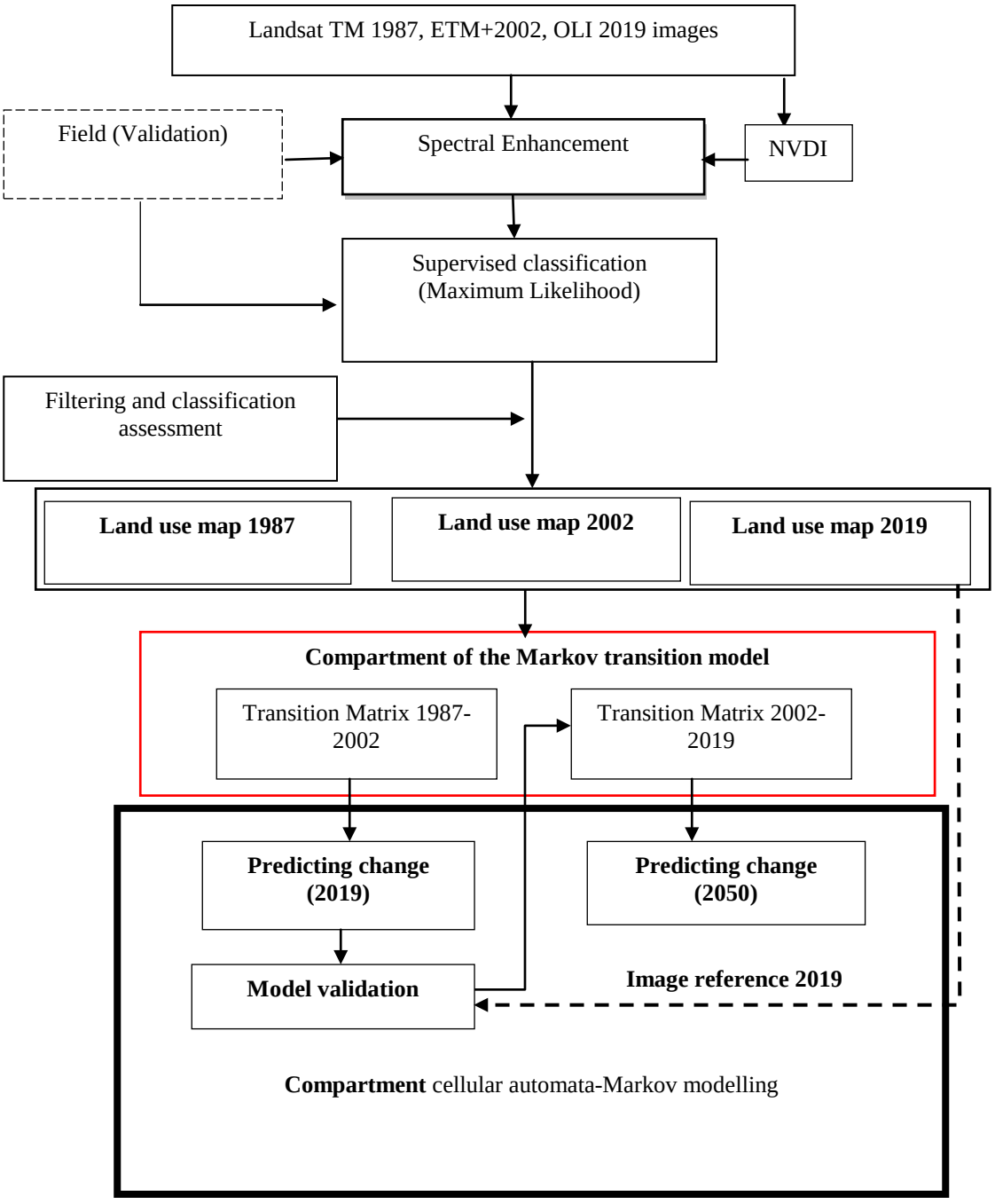

Fig. 2: Methodology used for land use monitoring

4. Results and discussions

4.1. Spectral Enhancement

Colour combination shown from image process were used to describe land cover types. This Landsat TM band 5, 4, 3 combination of TM images (Fig. 3) and ETM+ and 6-5-4 of the Landsat OLI-TIRS images provided the best discrimination of land cover types.

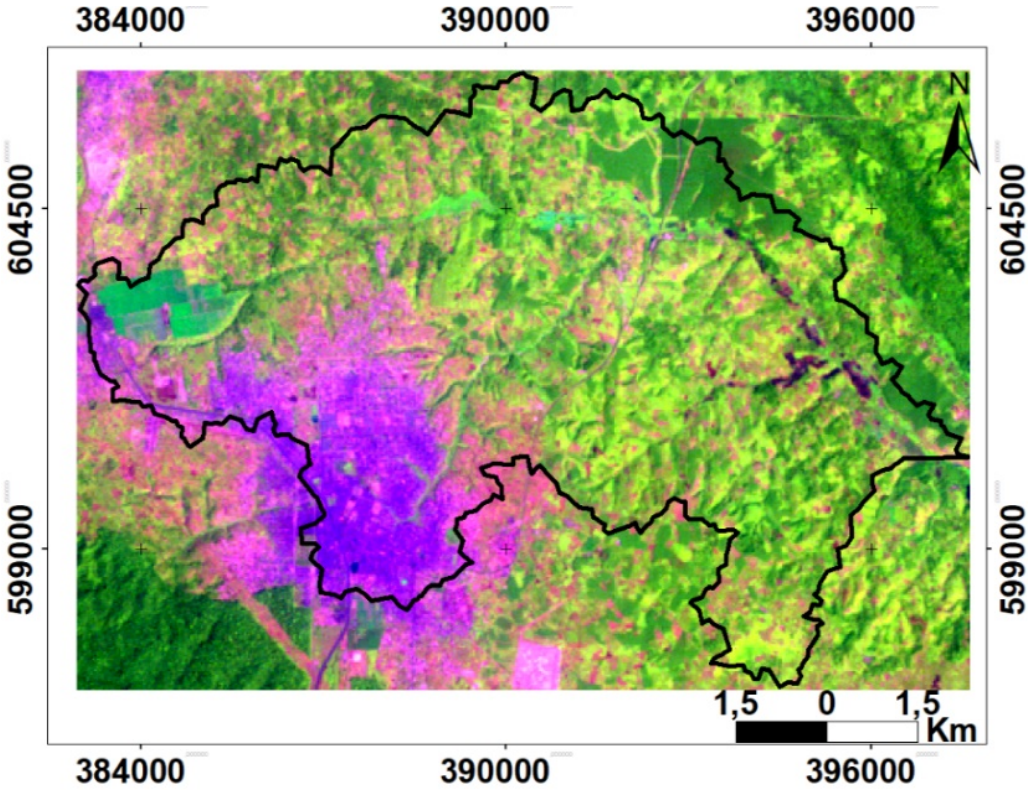

Fig. 3: TM 5-4-3 colour composition of 1987 Landsat image of the Djibi watershed

Figure 3 shows that rubber plantations, palm tree + degraded forest are characterised by green color. habits are characterised by dark to light purple color. Food crops + fallow land are characterised by a mosaic of yellow to light green. Water bodies appear in light blue. Bare ground appears in white.

4.2. Classification validation

The different classifications were evaluated by the confusion matrices represented by Tables 1, 2 and 3 through the overall classification accuracy calculation and the Kappa coefficient. These tables show the percentage of well classified pixels on the diagonal and the percentage of poorly classified pixels off the diagonal.

Table 1: 1987 Landsat TM image classification's confusion matrix

Classes OCS	WA	HA	BG	RPPDF	FCFL
WA	**97,87**	0,05	0	0,76	0,08
HA	0	**91,67**	7,46	0	0,33
BG	0	8,06	**92,54**	0	0,01
RPPDF	0,8	0	0	**98,98**	0,25
FCFL	1,33	0,22	0	0,26	**99,33**
TOTAL	**100**	**100**	**100**	**100**	**100**

Overall accuracy = **96,43%** and kappa coefficient = **0.95%**

Legend: WA = water, **BG** = bare ground, **HA** = habitats, **RPPDF** = rubber plantations, palmer tree + degraded forest, **FCFL** = food crops + fallow land

Confusion matrix shows a good classification of the image. However, some confusions occurred. The most important are in these cases

- 7.46% of habitats confused with bare soil.
- 8.06% of bare soil is confused with habitats

Table 2: 2002 Landsat ETM+ image classification's confusion matrix

Classes OCS	WA	HA	BG	RPPDF	FCFL
WA	**100**	0,05	0	0,15	0
HA	0	**99,72**	0	0	1,45
BG	0	0,19	**98,85**	0	0,36
RPPDF	0	0	0	**99,69**	0
FCFL	0	0,04	1,15	0,16	**98,19**
TOTAL	**100**	**100**	**100**	**100**	**100**

Overall accuracy = **99.56%** and kappa coefficient **= 0.99%**

Legend: WA = water, **BG** = bare ground, **HA** = habitats, **RPPDF** = rubber plantations, palmer tree + degraded forest, **FCFL** = food crops + fallow land

Table 3 shows slight confusions of some classes. These are: 1.15% and 1.45% of food crops and fallow land confused with bare soil and habitats respectively.

Table 3 : 2019 Landsat OLI image classification's confusion matrix

Classes OCS	WA	HA	BG	RPPDF	FCFL
WA	**95**	0	0	0,77	0,09
HA	0	**99,18**	0	0,17	0,87
BG	0	0,59	**98,51**	0	2,18
RPPDF	5	0	0	**98,12**	1,14
FCFL	0	0,23	1,49	0,94	**95,72**
TOTAL	**100**	**100**	**100**	**100**	**100**

Overall accuracy = **97.93%** and kappa coefficient **=0.97%**

Legend: WA = water, **BG** = bare ground, **HA** = habitats, **RPPDF** = rubber plantations, palmer tree + degraded forest, **FCFL** = food crops + fallow land

In this case confusion matrix shows a good classification of image (Table III). Confusions are still observe between the different classes. These are on the one hand between bare soil and spaced buildings, between food crops and fallow land and spaced buildings and on the other hand between dense buildings and spaced buildings.

- 1.14% of rubber, palm and degraded forest plantations were confused with food crops and fallow land.
- 1.49% of food crops and fallow land that were confused with bare soil.

Beyond the observed confusion, we can state that the classification obtained is good insofar as a classification is considered acceptable when the overall accuracy is around 80% [6] and [15]. The greatest confusion were significant between the habitat classes and bare soil. This can be explained separately, as these classes behave radiometrically in the same way and therefore have visually similar spectral responses.

4.3. Land use dynamics analysis

1987, 2002 and 2019 land use maps from Landsat TM, ETM+ and OLI images classification are presented in Figure 4. From 1987 to 2002, we observe a decreases in water areas, rubber plantations, palm trees and degraded forests, and food crops and fallow land, which go from 6.76% to 4.81%; from 25.05% to 19.71% and 47.81% to 38.54% respectively (Table 4 and Figure 4). Otherwise, we observe an increase in the habitat class from 17.62% to 31.69% and in bare soil from 2.76% to 5.25%. From 2002 to 2019, we also note the same decrease trends in the water class, rubber plantations, palm trees and degraded forests, and food crops and fallow land, which respectively go from 4.81% to 2.15%; from 19.71% to 17.87% and from 38.54% to 32.21%. And an increase in bare soil from 5.25% to 5.45% and habitats from 31.69% to 42.32% (Table 4 and Fig. 4).

The table also shows the average annual rate of spatial expansion and the overall rate of change from 1987 to 2002 and from 2002 to 2019. The same trends emerge from the analysis of the table, an annual decrease in water class, rubber plantations, palm and degraded forests and food crops/fallow and an increase in habitats and bare soil in the Djibi catchment. This fact is noted in studies by [32] and [7] who state that urbanisation and the agriculture extension contribute to increase in bare soil. and impermeability of soil, which results in an increase in surface runoff.

ISSN (Online) 2348 – 7968 | Impact Factor – 6.72

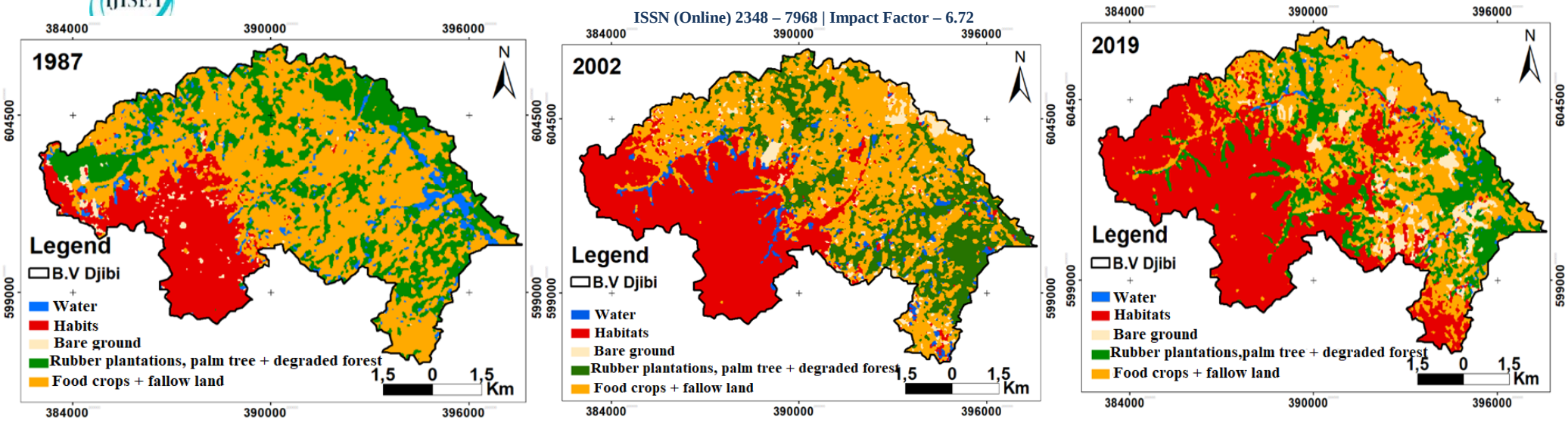

Fig. 4 :1987, 2002 et 2019 Land use map

Table 4: 1987, 2002 and 2019 land use classes Percentage

Land Use Class	Area (%)			AS (%)			OC (%)		
	1987	**2002**	**2019**	**1987-2002**	**2002-2019**	**1987-2019**	**1987-2002**	**2002-2019**	**1987-2019**
WA	6,76	4,81	2,15	-2,24	-4,63	-3,52	-28,86	-55,3	-68,2
HA	17,62	31,69	42,32	3,99	1,72	2,78	79,85	33,54	140,18
BG	2,76	5,25	5,45	4,38	0,22	2,15	90,22	3,81	97,46
RPPDF	25,05	19,71	17,87	-1,59	-0,57	-1,04	-21,32	-9,39	-28,66
FCFL	47,81	38,54	32,21	-1,43	-1,05	-1,23	-19,39	-16,42	-32,63

AS: Average annual rate of spatial expansion, **OC**: Overall rate of change

4.4. Land use state Simulation

4.4.1. Model calibration and validation

For the calibration, a transition probability matrix was produced using the land cover classes between 1987 and 2002 to be used as a basis for the land cover projection in 2019. The Markov matrix between 1987 and 2002 (Table 5) indicates the probability of each class in 2002 to migrate to another class or to remain stable in 2019.

Table 5: Transition probability matrix for the 2019 simulation

2002 1987	WA	HA	BG	RPPDF	FCFL
WA	**0,0582**	0,1526	0,0441	0,3037	0,4413
HA	0,0025	**0,9888**	0,0006	0,001	0,0071
BG	0,0084	0,9306	**0,0025**	0,0181	0,0404
RPPDF	0,0423	0,1453	0,0507	**0,2905**	0,04712
FCFL	0,0404	0,1937	0,043	0,2004	**0,5225**

Legend: WA = water, **BG** = bare ground, **HA** = habitats, **RPPDF** = rubber plantations, palmer tree + degraded forest, **FCFL** = food crops + fallow land

The transition matrix obtained gives the probability of change from one land use class to another. Thus, the 'Bare soil' class has the lowest probability of no change, i.e. 0.0025, it is therefore the most unstable class. This class is largely transformed into habitats at 93.06%. After the 'Bare soil' class comes the 'Plantations and degraded forests' class with a probability of no change of 0.2905. This is followed by food crops and fallow land at 0.5225.

This indicates a high level of human activity in the area. Plantations and degraded forests, food crops and fallow land are changing more into habitats (14.53%) and (19.37%) than bare soil (5.07%) and (4.3%). The habitat class is the most stable with a probability of no change of 0.9888. However, the probability magnitude shows that habitats are the most stressed. It is in demand because of the need for space as the population increases.

For model calibration, the simulated land use map in 2019 was validated by comparing it with the land use map of 2019 from the classification as shown in Figure 5.

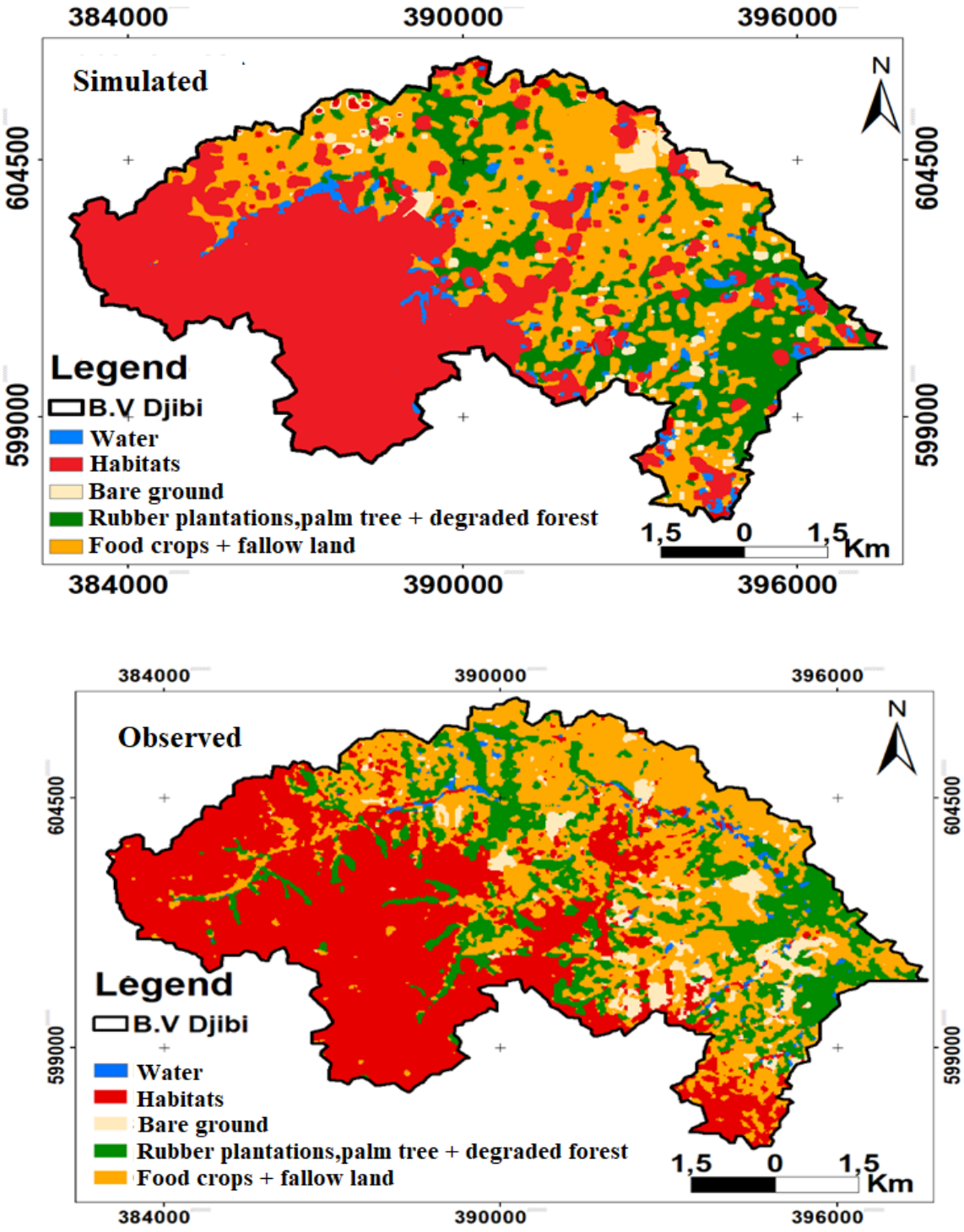

Fig. 5: Simulated and observed land use maps of 2019

Figure 6 below shows the different areas of the simulated 2019 map and the actual 2019 map.

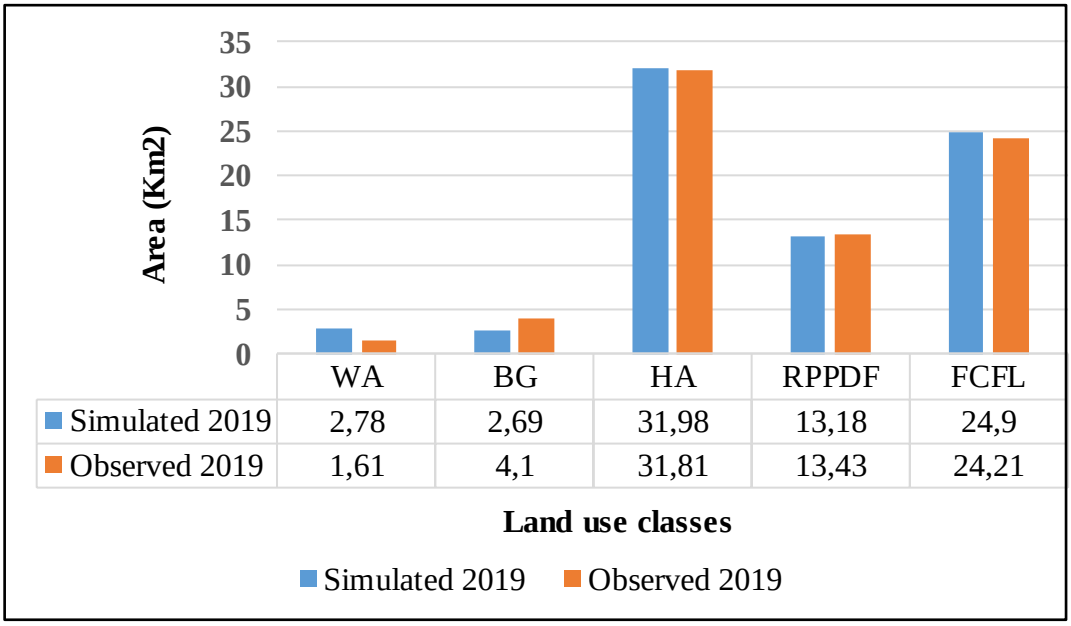

Fig. 6: Comparison between the simulated map and the real map of 2019

Legend: WA = water, **BG** = bare ground, **HA** = habitats, **RPPDF** = rubber plantations, palmer tree + degraded forest, **FCFL** = food crops + fallow land

Apart from "Water and bare soil" classes, there is no significant difference between the real and simulated data of the other classes. Both maps (simulated and real) show perfect similarities between the land use classes. Then we validated the model according to the global Kappa, Cramer's index, "Cramer's V" (degree of distribution or homogeneity of each class) and the categorical Kappa KIA, "Kappa Index Agreement" [27]. The categorical Kappa is 0.87 with a Cramer's coefficient of 0.81. Indeed, according to [27], Kappa values above 0.50 indicate a good agreement between the "real" and the simulated map; the results are good and usable. Also, according to [10.], when the Cramer coefficient is greater than 0.4 the distribution of thematic units (classes) are considered good. These indices give the possibility of any future predictions, including that of 2050.

4.4.2. Simulation of land use in 2050

After model calibration and assessing validity, it was interesting to examine the structure and trend change at a later date (2050). The prediction of the land cover in 2050 was made on the basis of the transition between 2002 and 2019 land covers. The result of the land cover prediction for 2050 is shown in Figure 7.

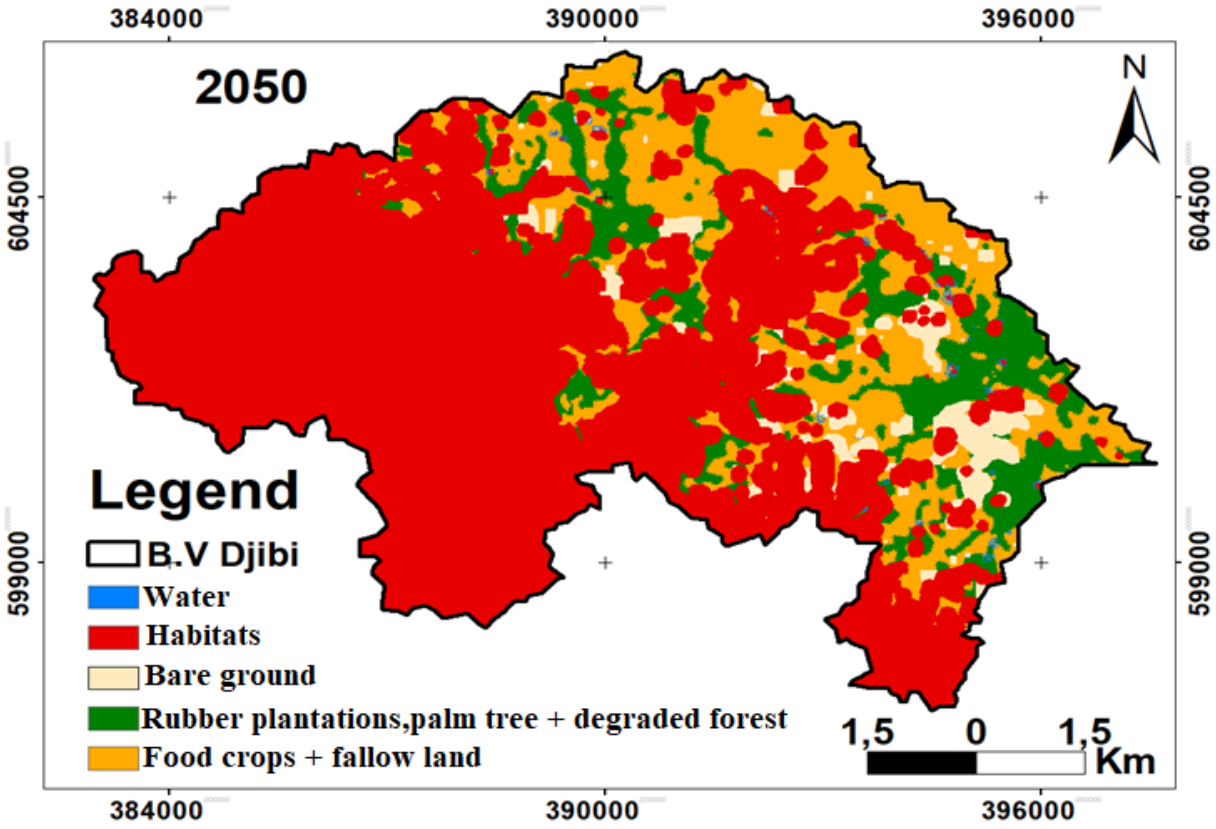

Fig. 7: 2050 land use map simulated

Visual analysis of simulation for 2050 shows that habitats will have a very high growth rate in favour of agricultural and vegetated surfaces. Water will decrease very strongly as shown in figure 7.

This trend would be due to anthropogenic pressures and population increase in the Djibi catchment. This is in line with the study undertake by [1.] in Punjab, a province of Pakistan, which explains the high demand for cultivated land and buildings due to increase of population. The decrease of water surfaces in the catchment area can be explained by the important silting up of the rivers due to anthropisation and agricultural activities in the high areas.

Finally, the CA_Markov model is an important decision-making tool for decision-makers, stakeholders and planners, as it allows us to understand and show the future of territories in the future

5. Conclusion

GIS and remote sensing using in land use modelling in the Djibi watershed led us to the IDRISI software, which is one of the software packages that fully integrates GIS and CA_Markov. This recent and innovative approach continues to prove itself within the scientific community.

Land use maps dynamic from supervised classifications of Landsat images (TM 1987, ETM+ 2002 and OLI 2019) has highlighted the challenges and threats to the ecological balance in the Djibi watershed in recent years. The cartographic results showed an annual decrease in the areas of plantations, crops and fallow land and water surfaces, respectively by 1.04%, 1.23% and 3.52% from 1987 to 2019. And a further annual increase of 2.78% for habitats and 2.15% for bare land from 1987 to 2019.

CA_Markov land use simulation predicted the land use in 2050 with an accuracy of 87%. It showed that the current trends of decreasing water class, agricultural and vegetated areas will continue in the future.

Acknowledgements

The authors would like to thank the Ivorian Direction of human hydraulic infrastructures (DGIHH) for providing hydrometric data, and the host Laboratory of Soil, Water and Geomaterials (LSSEEG) of Felix Houphouët Boigny University and UFR Marine Sciences (UFR-SDM) of the University of San Pedro.

References

[1.] Abdus. S., Xiangzheng. D., Siqi. J. et Dongdong. C. (2017). Scenario based simulation on dynamics of Land-Use change in Punjab province, Pakistan. *MDPI Sustainability*, Vol 9, N°1285, pp. 2- 17 P.

[2.] Akognongbe A., Abdoulaye D., Vissin. E. W et Boko.M. (2014). Dynamique de l'occupation du sol dans le bassin versant de l'Ouémé à l'exutoire de Bétérou (Bénin). *Afrique SCIENCE* 10 (2) pp. 228 – 242.

[3.] Batchi M., Karkouri J.A., Fenjiro I, Maaqili M. E. (2017). Étude comparative de deux modèles (DRASTIC et SI) pour l'évaluation de la sensibilité de la nappe phréatique de Mnasra (Maroc nord-occidental) à la pollution d'origine agricole. *Physio-Géo*. Vol.11, pp. 43-64. https://doi.org/10.4000/physio-geo.5213.

[4.] Benmessaoud H., Kalla M. et Driddi H. (2008). Évolution de l'occupation des sols et désertification dans le Sud des Aurès (Algérie). *Mappemonde*, N° 94, pp. 1-10.

[5.] Chen, H. et Pontius, R. G. (2010). Diagnostic tools to evaluate a spatial land change projection a long a gradient of an explanatory variable. *Landscape Ecology*, 25: pp. 1319- 1331.

[6.] Congalton, G. R. (1991). A Review of Assessing the Accuracy of Classifications of Remotely Sensed Data. *Remote Sensing of Environment*. Vol. 46 : pp. 35-37.

[7.] Diallo S., Noufé D., Tra B. Z. A., Dao A., Kamagaté B., Effebi K. R., Goné Droh Lanciné, Jean. E. P., Jean-Luc. P, Luc S. (2018). Effets de la dynamique du couvert végétal sur les écoulements dans le bassin versant de la lagune Aghien en côte d'ivoire *European Scientific Journal*, Vol.14, N°.36 pp.1857- 7431.

[8.] Dodane C., Joliveau T. et Riviere H. A. (2014)."Simuler les évolutions de l'utilisation du sol pour anticiper le futur d'un territoire", Cybergeo *: European Journal of Geography*, N°689, pp. 245-260.

[9.] Eastman J. R. (2006). IDRISI andes. Guide to GIS and Image Processing. *Worcester, Clark University*, 457 p.

[10.] Eastman J.R. (2015). TerrSet manual. Clark Lab. 392 p.

[11.] FAO. (1996). *Forest resources assessment 1990 - Survey tropical forest cover studies of change processes.* FAO Forestry Paper 130, Food and Agriculture Organization of United Nations, Rome, Italie. [en ligne] http://www.fao.org/docrep/007/w0015e/w0015e00.htm.

[12.] FAO. (2011). *Situation des forêts du monde.* Rapport principal, Organisation des Nations Unies pour l'alimentation et l'agriculture (FAO), Rome, Italie. 193 p.

[13.] FAO. (2016). La situation mondiale de l'alimentation et de l'agriculture. Rapport principal, Organisation des Nations Unies pour l'alimentation et l'agriculture. Rome, (FAO), Rome, Italie.214 p.

[14.] Geist, H. J. et Lambin, E. F. (2001). What Drives Tropical Deforestation? A meta-analysis of proximate and underlying causes of deforestation based on subnational case study evidence. *LUCC Report Series*, N° 4, 136 p.

[15.] Girard, M. C. et Girard, C. M. (1999). Traitement des données de télédétection. *Dunod*, Paris,529 p.

[16.] Griffith J. A. et Alii (2003). «Detecting trends in landscape pattern metrics over a 20-year period using a sampling-based monitoring programme». *International Journal of Remote Sensing*, Vol. 24, pp. 175-81.

[17.] Hadjadj M. F. (2011). Apport des SIG et des images satellites pour la cartographie numérique de la forêt du Chettabah (Wilaya de Constantine) : Modélisation climatique et classification. Mémoire de fin d'études, Université El-Hadj Lakhdar Batna, Constantine, Algérie. 178 p.

[18.] Houet T. (2006). Occupation des sols et gestion de l'eau : Modélisation prospective en paysage agricole fragmenté (Application au SAGE du Blavet). Thèse de Doctorat, Université de Rennes 2 Haute Bretagne, 357 p.

[19.] Koffi E S., Dao A., Noufé D.D., Kamagaté B., Koffi J T., Diallo S., et Goné D. L. (2018). Bilan des apports liquides des rivières Bété et Djibi a la lagune Aghien (Côte d'Ivoire). *Am. J. innov. res. appl. sci.* Vol. 6, N°2, pp. 86-99.

[20.] Koné M., Aman A., Yao A. C., Coulibaly L. et N'guessan K. E. (2007). Suivi diachronique par télédétection spatiale de la couverture ligneuse en milieu de savane soudanienne en Côte d'Ivoire. *Revue Télédétection*, Vol. 7, N° 1, pp. 433-446.

[21.] Lagabrielle E., Metzger P., Martignac C., Lortic B. et Durieux Laurent (2007). Les dynamiques d'occupation du sol à la Réunion (1989-2002). *Mappemonde* N°86, pp. 23.

[22.] Lu, D. et Alii (2004). « Change detection, technic», International Journal of Remote Sensing, Vol. 25, N°12, pp. 2365-2407.

[23.] Mas J.F. (2000). « Une revue des méthodes et des techniques de télédétection du changement », *Journal canadien de télédétection.* Vol. 26, N°4, pp. 349- 362.

[24.] Moghadam H. S., et Helbich M. (2013). Spatiotemporal urbanization processes in the megacity of Mumbai, India: A Markov chains-cellular automata urban growth model. *Elsevier*, Vol 40, pp. 140-149. https://doi.org/10.1016/j.apgeog.2013.01.009.

[25.] Myint, S.W. et Wang, L. (2006). Multicriteria decision approach for land use and land cover change using Markov chain analysis and a cellular automata approach. *Canadian Journal of Remote Sensing*, 32 : pp. 390-404.

[26.] N'guessan E., Dibi N'da H., Bellan M.-F. et BLASCO F. (2006). Pression anthropique sur une réserve forestière en Côte d'Ivoire : Apport de la télédétection. *Revue Télédétection*, Vol. 5, N°4, pp. 307-323.

[27.] Nghiem V.T. (2014). Impact du changement du mode d'occupation des sols sur le fonctionnement hydrogéochimique des grands bassins versants : cas du bassin versant de l'Ain. Thèse de Docteur de l'Université de Grenoble, 306 p.

[28.] Oszwald J. (2005). Dynamique des formations agroforestières en Côte d'Ivoire (des années 1980 aux années 2000) : Suivi par télédétection et développement d'une approche cartographique. Thèse de doctorat, Université des Sciences et Technologies de Lille, France. 304 p.

[29.] Pontius J. R. G. (2000). Quantification error versus location error in comparison of categorical maps. Photogrammetric Engineering and remote sensing, Vol 66, N°8, pp. 1011- 1016.

[30.] Pontius R.G. et Malanson J., (2005). Comparison of the structure and accuracy of two land change models. *International Journal of Geographical Information Science*, Vol 19, N°2, pp. 243-265.

[31.] Sanga L., Zhanga C., Yanga J., Zhua D. and Yun W (2011). Simulation of land use spatial pattern of towns and villages based on CA–Markov model. Vol 54, Issues 3–4, August 2011, pp 938-943. https://doi.org/10.1016/j.mcm.2010.11.019

[32.] Yao B. A., K. I. Kouamé, K. A. Kouassi, K. Kouadio, B. T. A. Goula et I. Savané, (2015). Estimation de la recharge d'une nappe côtière en zone tropicale humide : cas de la nappe du continental Terminal d'Abidjan (Côte d'Ivoire). *International Journal Innovation and Applied Studies*, vol. 12, no. 4, pp. 888-898.